Enhanced Radio Frequency Field Penetration in an Inductively Coupled Plasma

M. Tuszewski
Los Alamos National Laboratory, Los Alamos, New Mexico 87545
(Received 11 March 1996)

The induced radio frequency magnetic fields of a low-frequency inductively coupled plasma are measured and modeled. The fields penetrate deep into the discharge, in contrast with existing predictions of field decay within a thin skin layer. Fluid calculations show that the enhanced penetration is due to a reduction of the plasma conductivity by the induced magnetic fields. [S0031-9007(96)00766-1]

PACS numbers: 52.40.Db, 52.50.Gj, 52.80.Pi

Inductively coupled plasmas (ICPs) consist of a dielectric chamber surrounded by a conducting coil [1]. Radio frequency (rf) power continuously applied to the coil induces electric fields that partially ionize a gas inside the chamber and sustain a discharge. ICPs have in the past been operated with high (1–760 Torr) gas pressures for thermal [2] and lighting [3] applications. Recently, ICPs have been rediscovered by the semiconductor and other industries as an important class of high-density (10^{11}–10^{12} cm^{-3}), low-pressure (1–10 mTorr) plasma sources [4]. Present low-pressure ICP development [5–10] and modeling [11–16] are among the most active areas of plasma research.

The understanding of rf power absorption is fundamental to ICP heating and transport properties. These properties must be accurately described in ICP models to predict plasma radial uniformity, a crucial issue for future large-area processes. In present models that consider induced rf electric (but not magnetic) fields, the rf power is transferred to plasma electrons within a skin layer near the plasma surface [2–4,11–16]. The electron heating is either collisional (Ohmic) or collisionless (stochastic) [12,16]. For typical rf frequencies of 0.1–13.56 MHz, the skin depths are a few cm while device dimensions are 10–30 cm. The ICPs can be cylindrical [2,3,5], planar [6–9], or hemispherical [10]. The measured skin depths are consistent with the above models [2,3,7].

In this Letter, data are presented that show deep rf penetration into argon ICP discharges. For these data, stochastic effects are unimportant and collisional skin depths are small. Hence, a new mechanism must be invoked to explain the enhanced rf field penetration. Fluid calculations suggest that this mechanism is a reduction of the plasma conductivity by the induced rf magnetic fields when the electron cyclotron angular frequency ω_c exceeds the rf angular frequency ω and the electron-neutral collision frequency ν. This condition is satisfied for many low-pressure ICPs. Hence, the induced rf magnetic fields must be included in ICP models to predict electron heating and the resulting plasma transport. The influence of rf magnetic fields on ICP density profiles (the ponderomotive effect) has already been identified [17–19].

The induced rf magnetic fields are measured inside a cylindrical ICP sketched in Fig. 1. A 13-turn copper coil is wound around a glass bell jar of inner radius $R = 16.5$ cm. The coil is powered by a 2 kW, 0.46 MHz ($\omega = 2.9$ megacycle), rf generator via a matching network. The experimental apparatus is detailed elsewhere [10]. A small pickup coil (18 turns, 4 mm diameter, 5 mm length) with shielded twisted leads is inserted near the closed end of a 6 mm diameter ceramic tubing. This tubing is connected to a stainless steel shaft via ceramic transition pieces shown in Fig. 1. The pickup coil is oriented to measure the z (upward) component of the induced rf magnetic field. Radial scans are obtained in the coil midplane ($z = 0$) by rotating the steel shaft.

The pickup coil, calibrated at 0.46 MHz, has a sensitivity of 65 mV/G. This sensitivity is checked by measuring the vacuum rf magnetic fields inside the glass vessel and by comparing these data to numerical predictions based on 13 circular loops: Agreement within 3% is obtained. In another check, the pickup coil is rotated to a horizontal position to measure combined radial and azimuthal fields: These fields are found negligible at $z = 0$, with and without plasma. The coil current and the coil voltage around the three turns closest to $z = 0$ are also measured. The latter yields an estimate for the coil azimuthal electric field E_c at $z = 0$. Uncertainties in the magnetic and electric field measurements are (5–10)%.

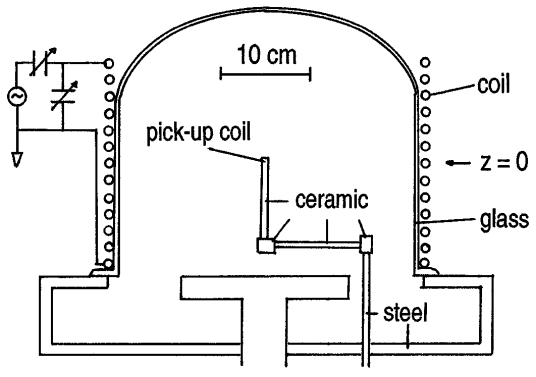

FIG. 1. Sketch of the inductively coupled plasma.

 0031-9007/96/77(7)/1286(4)$10.00

Argon discharges are sustained with gas pressures of 5–50 mTorr and with rf powers of 0.5–1.5 kW. The radial profiles of ion density obtained from a voltage-swept cylindrical Langmuir probe [10] are shown in Fig. 2 for 5 mTorr argon discharges. The magnitude of the ion density is checked by two methods. First, both electron and ion densities are estimated from their respective saturation currents [20]: Ratios $n_i/n_e \sim 1.5$–2.0 are consistently obtained. This reasonable agreement is expected in the thin sheath regime (mean free path $\gg$ probe radius $\gg$ Debye length). Second, a 35 GHz microwave interferometer is used along a diameter at $z \sim -10$ cm, with the ICP coil lifted by 5 cm. The values of $\int n_e\, dr$ from the interferometer are compared to the values of $\int n_i\, dr$ from probe radial profiles at the same z location: Ratios $\int n_i\, dr / \int n_e\, dr \sim 1.1$–$1.3$ are obtained. The ion densities in Fig. 2 are probably accurate with 30%.

The electron temperatures T_e are also estimated from Langmuir probe data. For the discharges of Fig. 2, T_e increases from 2.4 to 2.6 eV with rf power. The T_e profiles are radially uniform and the electron energy distributions are close to Maxwellians. The collision frequency is calculated as $\nu = KN$, where K is the argon elastic rate [4] and N is the neutral gas density that corresponds to a temperature of 300 K. These values of ν agree within 10% with those used in other ICP experiments [8,9] and models [4,13,15,16]. The collision frequencies may be somewhat overestimated because probe-determined T_e values tend to be too high and because higher gas temperatures are likely.

The measured magnitudes $|B|$ of the induced rf magnetic field B_z are shown with symbols in Fig. 3 for 5 mTorr argon discharges. The $|B|$ profiles are quite flat near the wall and change curvature at smaller radii. The magnitudes of $|B|$ and E_c increase with rf power. The measured E_c are 53, 72, and 81 V/m for the discharges of Fig. 3.

The magnetic field data are first compared to the predictions from existing models. A fluid approach is used to describe the ICP discharges. The electron momentum equation is

$$mn[\partial/\partial t + \mathbf{v}\cdot\nabla]\mathbf{v} = -ne(\mathbf{E} + \mathbf{v}\times\mathbf{B}) - \nabla p - nm\nu\mathbf{v}, \qquad (1)$$

where bold quantities are vectors. The last term accounts for electron-neutral collisions with a constant ν. The smaller electron-ion collision term is neglected. The plasma conductivity σ is derived assuming axisymmetry and v, $E \sim e^{i\omega t}$. One obtains $v_\theta = -eE/m/(\nu + i\omega)$ from the azimuthal component of Eq. (1), neglecting convective ($\mathbf{v}\cdot\nabla\mathbf{v}$) and magnetic ($\mathbf{v}\times\mathbf{B}$) terms. Then, σ is calculated by inserting the plasma current, $j = -nev_\theta$, into Ohm's law, $j = \sigma E$. One obtains the ubiquitous expression [3–5,11–16]

$$\sigma = ne^2/[m(\nu + i\omega)]. \qquad (2)$$

A one-dimensional model, with $B = B_z(r)$, is used for simplicity. Although it strictly applies only to infinitely long ICPs, this model is adequate for comparison with data obtained at $z = 0$ where $\partial B_z/\partial r \gg \partial B_r/\partial z$. Eliminating E from Faraday's law, $(1/r)(d/dr)rE = -i\omega B$, by using Ohm's law and Ampere's law, $dB/dr = -\mu_0 j$, one obtains [3]

$$(1/r)(d/dr)(r/\sigma)\, dB/dr = i\omega\mu_0 B, \qquad (3)$$

where B and σ are complex quantities. For constant density, Eqs. (2) and (3) yield skin depths that increase from $\delta_p = c/\omega_p$ for $\omega \gg \nu$ (c is the speed of light and ω_p is the plasma frequency) to $\delta_c = \delta_p(2\nu/\omega)^{1/2}$ for $\nu \gg \omega$.

For variable densities, Eq. (3) must be solved numerically by separating real and imaginary parts. The resulting two, coupled, second-order, ordinary differential

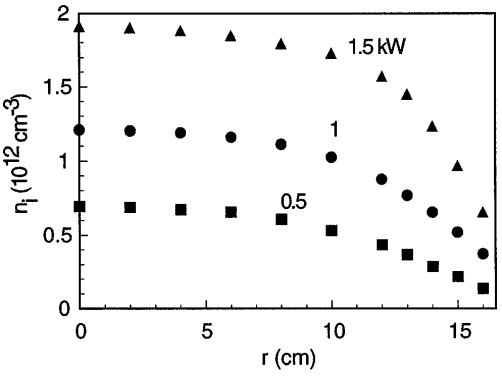

FIG. 2. Measured radial profiles of ion density for argon discharges with 5 mTorr gas pressure and with 0.5, 1, and 1.5 kW rf power.

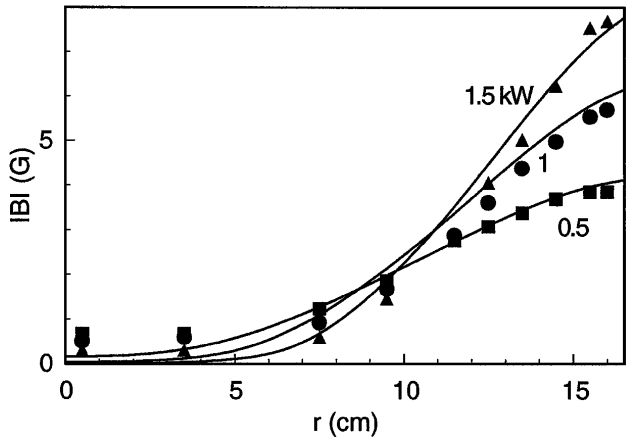

FIG. 3. Radial profiles of rf magnetic field amplitude for 5 mTorr argon discharges. The measured data are indicated with symbols. The magnetized calculations are shown with solid lines.

equations are integrated numerically with σ from Eq. (2) and with polynomial fits to the density data of Fig. 2. The following boundary conditions are used at $r = 0$: $dB_r/dr = dB_i/dr = 0$, and $B_i = 0$ (subscripts refer to real and imaginary components). $B_i(0) = 0$ can always be chosen as a phase angle reference. $B_r(0)$ is found by successive iterations such that $|E|$ at the coil, obtained from integrating Faraday's law, is equal to the measured E_c.

The calculated radial $|B|$ profiles are shown in Fig. 4 with solid curves. The data are also shown with symbols for comparison. The calculated $|B|$ magnitudes and decays are overestimated by factors of 2 to 3. In addition, the exponential-like calculated profiles do not reproduce the change of curvature observed near the wall. The uncertainties in the calculated penetration depths δ_c from n, ν, and the one-dimensional approximation are estimated to be about 40%. These uncertainties do not explain the above discrepancies. Clearly, a better model is required.

The largest term of Eq. (1) that has been neglected in obtaining Eq. (2) is the magnetic term. Dimensional analysis shows that the ratios of convective to magnetic terms are of order $\delta_p^2/(r\delta)$, typically a few percent [$\delta = B/(dB/dr)$]. The magnetic term introduces a nonlinearity in Eq. (1) where v, B, and E must now be described by harmonic series ($\sum_k e^{ik\omega t}$). Substantial harmonics are observed, especially at high rf powers, in the rf magnetic field wave forms, in the Langmuir probe currents, and in the coil voltages [10]. The latter occur because ICPs are similar to electrical transformers [4].

Fourier analysis can be used to solve Eq. (1), but this approach is not particularly enlighting. Since the lowest harmonic still dominates the rf wave forms, a simpler approach might be to define an effective conductivity $\langle\sigma\rangle$ that is time averaged over an rf period. With $\partial/\partial t \sim i\omega$, v_r can be eliminated from the θ and r components of Eq. (1) to obtain v_θ. Then, σ is derived as before and is averaged over an rf period with $\omega_c = eB/m = |\omega_c|\sin(\omega t)$. Assuming $\omega < \nu < |\omega_c|$ and retaining terms of order ω/ν, one obtains

$$\langle\sigma\rangle = \sigma_0/(1 + |\omega_c|^2/\nu^2)^{1/2} - i\sigma_0(\omega/\nu)/(1 + |\omega_c|^2/\nu^2)^{3/2}, \quad (4)$$

where $\sigma_0 = ne^2/(m\nu)$ is the zero-frequency collisional conductivity. The small imaginary term is included only to recover the unmagnetized limit when $|\omega_c| < \nu$. When $|\omega_c| > \nu$, $\langle\sigma\rangle \sim ne^2/(m|\omega_c|)$ is reduced by $\nu/|\omega_c|$ compared to σ_0 and $\delta_b \sim \delta_p(2|\omega_c|/\omega)^{1/2}$ is increased by $(|\omega_c|/\nu)^{1/2}$ compared to the unmagnetized skin depth $\delta_c \sim \delta_p(2\nu/\omega)^{1/2}$.

Equation (3) is solved as before, but with $\langle\sigma\rangle$ from Eq. (4). The calculated $|B|$ profiles are shown in Fig. 3 with solid curves. The calculated and observed $|B|$ magnitudes agree with 5% near the wall. The calculations also reproduce the shape of the observed profiles. The edge flattening and the change in profile curvature are due to low edge plasma conductivities $\langle\sigma\rangle$. The sharp boundary channel model [21] roughly approximates the present conductivity profiles. The magnetized calculations are independent of ν at large radii where $\langle\sigma\rangle \sim ne^2/(m|\omega_c|)$. Hence, the calculated depths δ_b have relatively small (20%) uncertainties.

The measured and calculated $1/e$ decay lengths (from edge values) of the $|B|$ profiles are shown in Fig. 5 for the 5 mTorr argon discharges. The error bars are the estimated uncertainties. The magnetized depths δ_b agree with the measured depths δ in all cases. The unmagnetized depths δ_c are too small by factors of 2 to 3. The stochastic (anomalous) skin depths [12] $\delta_s \sim \delta_p[v_e/(2\omega\delta_p)]^{1/3}$, where $v_e = [8kT_e/(\pi m)]^{1/2}$,

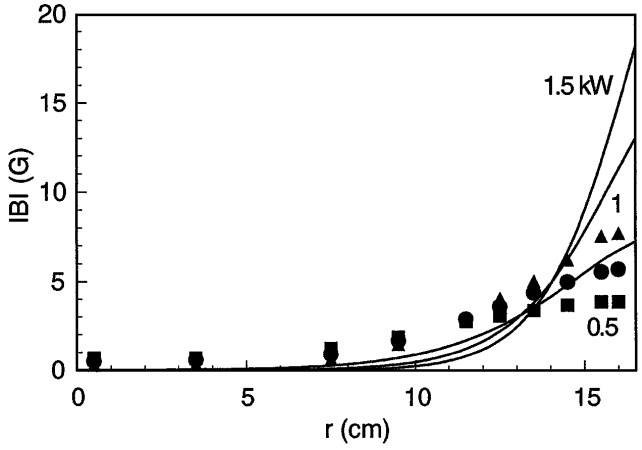

FIG. 4. Radial profiles of rf magnetic field amplitude for 5 mTorr argon discharges. The measured data are indicated with symbols. The unmagnetized calculations are shown with solid lines.

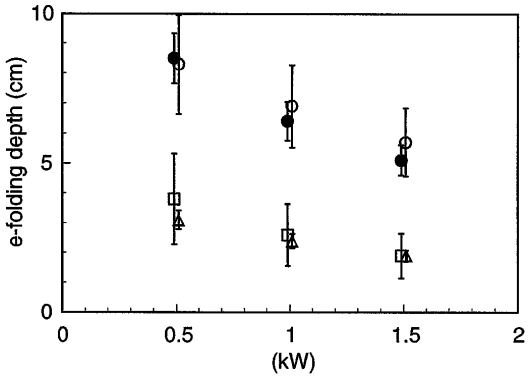

FIG. 5. Measured and calculated rf magnetic field penetration depths as functions of rf power for 5 mTorr argon discharges. The measured depths δ are shown with solid circles, the magnetized depths δ_b are shown with open circles, the unmagnetized depths δ_c are shown with squares, and the stochastic depths δ_s are shown with triangles.

are smaller or comparable to the δ_c values, so that stochastic effects are unimportant. In addition, these unmagnetized δ_s estimates are probably too large for the present discharges where the electron radial motion is inhibited by the rf magnetic field. The electron magnetization in the edge region where penetration depths are calculated also extends the validity of the fluid approach down to pressures of a few mTorr.

The $|B|$ profiles are also measured for argon discharges with higher (10–50 mTorr) gas pressures. The magnetized calculation agrees with the data for all pressures. The discrepancy between the unmagnetized calculation and the data gradually diminishes as the gas pressure increases. Data and both calculations coincide within uncertainties for 40 and 50 mTorr discharges. This agreement is expected since $\langle\sigma\rangle \sim \sigma$ for high-pressure discharges where ν exceeds $|\omega_c|$ through most of the plasma volume. The agreement between data and calculations also implies that the combined experimental uncertainties are less than a factor of 2.

The $|B|$ profiles of oxygen discharges are also measured and calculated. These discharges, more representative of industrial ICPs, yield qualitatively similar results as for argon, except that the rf penetration depths are larger by factors of 2–3 because of lower plasma densities. The rf magnetic fields of the oxygen discharges are 1–3 G on axis. Hence, the plasma conductivity is substantially reduced by the rf magnetic field at all radii.

Although cases with $|\omega_c| > \omega > \nu$ were not investigated experimentally, numerical averages of σ over an rf period suggest that Eq. (4) remains a good approximation whenever $|\omega_c| > \omega, \nu$, regardless of the ordering of ω and ν. Hence, the ICP rf power absorption depends on the largest of ω, ν, $|\omega_c|$, and the effective stochastic frequency ν_s. The skin depths are (1) δ_p for high (13.56 MHz) rf frequencies and low rf powers where ω dominates [8], (2) $\delta_c \sim \delta_p(2\nu/\omega)^{1/2}$ for high pressure ICPs where ν dominates [2,3], (3) $\delta_b \sim \delta_p(2|\omega_c|/\omega)^{1/2}$ for the present ICPs where $|\omega_c|$ dominates, and (4) δ_s for low-pressure ICPs if ν_s dominates.

The regime where $|\omega_c|$ is largest has been overlooked until now. The induced rf magnetic fields are only 3–10 G for typical rf powers and seem negligible. Hence, they are usually neglected in ICP models [11–16]. However, the corresponding values $|\omega_c| \sim 50$–180 are often larger than typical values $\nu \sim 5$–20 and $\omega \sim 1$–85 (megacycle). Hence, the rf penetration depths δ are often substantially increased by the rf magnetic field and the Ohmic heating power densities ($\sim 1/\delta^2$) can be reduced by an order of magnitude.

In summary, the induced rf magnetic fields of a low-frequency ICP show substantial penetration while existing models predict absorption in a thin skin layer. Fluid calculations resolve this apparent contradiction: The induced rf magnetic fields appreciably reduce the plasma conductivity, which leads to a larger rf penetration. The rf magnetic fields can significantly modify electron heating and the resulting plasma transport in many of today's low-pressure ICPs, and should therefore be included in future ICP models.

This research was conducted under the auspices of the U.S. DOE, supported by funds provided by the University of California for discretionary research by Los Alamos National Laboratory.

[1] W. Hittorf, Wiedemanns Ann. Phys. **21**, 90 (1884).
[2] H. U. Eckert, High Temp. Sci. **6**, 99 (1974).
[3] J. W. Denneman, J. Phys. D **23**, 293 (1990).
[4] M. A. Lieberman and A. J. Lichtenberg, *Principles of Plasma Discharges and Materials Processing* (John Wiley, New York, 1994).
[5] V. A. Godyak, R. B. Piejak, and B. M. Alexandrovich, Plasma Sources Sci. Technol. **3**, 169 (1994).
[6] J. S. Ogle, U.S. Patent No. 4,948,458 (1990).
[7] J. H. Keller, J. C. Forster, and M. S. Bames, J. Vac. Sci. Technol. A **11**, 2487 (1993).
[8] J. Hopwood, C. R. Guarnieri, S. J. Whitehair, and J. J. Cuomo, J. Vac. Sci. Technol. A **11**, 147 (1993).
[9] L. J. Mahoney, A. E. Wendt, E. Barrios, C. J. Richards, and J. L. Shohet, J. Appl. Phys. **76**, 2041 (1994).
[10] M. Tuszewski and J. A. Tobin, J. Vac. Sci. Technol. A **14**, 1096 (1996).
[11] P. L. G. Ventzek, T. J. Sommerer, R. J. Hoekstra, and M. J. Kushner, Appl. Phys. Lett. **63**, 605 (1993).
[12] M. M. Turner, Phys. Rev. Lett. **71**, 1844 (1993).
[13] R. A. Stewart, P. Vitello, and D. B. Graves, J. Vac. Sci. Technol. B **12**, 478 (1994).
[14] A. P. Paranjpe, J. Vac. Sci. Technol. A **12**, 1221 (1994).
[15] G. DiPeso, V. Vahedi, D. W. Hewett, and T. D. Rognlien, J. Vac. Sci. Technol. A **12**, 1387 (1994).
[16] V. Vahedi, M. A. Lieberman, G. DiPeso, T. D. Rognlien, and D. Hewett, J. Appl. Phys. **78**, 1446 (1995).
[17] J. C. Helmer and J. Feinstein, J. Vac. Sci. Technol. B **12**, 507 (1994).
[18] G. DiPeso, T. D. Rognlien, V. Vahedi, and D. W. Hewett, IEEE Trans. Plasma Sci. **23**, 550 (1995).
[19] R. H. Cohen and T. D. Rognlien, Bull. Am. Phys. Soc. **40**, 1643 (1995).
[20] I. D. Sudit and R. C. Woods, J. Appl. Phys. **76**, 4488 (1994).
[21] M. P. Freeman and J. D. Chase, J. Appl. Phys. **39**, 180 (1968).